A Comparison of the Surface Pressure Distribution of Circular Cables and Helical Fillet Cables under Wind Attack: A Wind Tunnel Test Study

Duy Thao Nguyen
Faculty of Road and Bridge Engineering, The University of Danang – University of Science and Technology, Vietnam
ndthao@dut.udn.vn

Duy Hung Vo
Faculty of Road and Bridge Engineering, The University of Danang – University of Science and Technology, Vietnam
vdhung@dut.udn.vn

Viet Hai Do
Faculty of Road and Bridge Engineering, The University of Danang – University of Science and Technology, Vietnam
dvhai@dut.udn.vn (corresponding author)

Received: 23 April 2024 | Revised: 8 May 2024 | Accepted: 13 May 2024

 DOI: https://doi.org/10.48084/etasr.7602

ABSTRACT

This study examines the aerodynamic performance and surface pressure distribution features of circular and helical fillet stay cables when subjected to wind using wind tunnel testing. The research seeks to clarify the aerodynamic performance disparities between conventional circular stay cables and helical fillet cables, providing valuable insights into their appropriateness for cable-supported structures exposed to wind-induced vibrations. The study initially investigates the aerodynamic efficiency of circular and helical fillet cables. Afterward, the wind tunnel captures the distribution of surface pressure on both cable surfaces. The findings suggest that circular stay cables may undergo cable dry galloping, whereas helical fillet cables demonstrate stability when subjected to wind forces. Furthermore, there are noticeable differences in the surface pressure distribution patterns between circular stay cables and helical fillet cables. Circular stay cables provide a symmetric distribution of pressure, with uniform pressure magnitudes along their surfaces, forming a symmetric pattern. On the other hand, helical fillet cables exhibit modified airflow patterns, leading to asymmetric pressure on the cable surface. Furthermore, the dry galloping observed in circular cables is attributed to the presence of low-frequency components. In contrast, helical fillet cables exhibit a more regulated incidence of low-frequency vortices, making them less prone to wind-induced vibrations.

Keywords-surface pressure distribution; wind tunnel test; circular surface; helical fillet; symmetric distribution; asymmetric distribution

I. INTRODUCTION

An essential part in designing and analyzing cable-supported bridges and transmission lines is understanding how circular stay cables behave when subjected to wind loads. It is crucial to comprehend the distribution of surface pressure along these cables to guarantee their stability and safety while exposed to wind forces. Authors in [1-2] established the basis for comprehending vibrations caused by wind in cables, highlighting factors such as cable diameter and wind velocity as the main factors influencing the wire's reaction. Follow-up studies [3-8], further explored the aerodynamic properties of circular cables, emphasizing the importance of surface pressure distribution in impacting the structural response to wind loads. Historical records document occurrences of stay cables vibrating due to the interaction of rain and wind, both during

bridge building and after its completion [3, 9-12]. Recent studies have shown that cables can experience excitation even without rain, a phenomenon known as dry galloping [13-19]. In fact, the cable vibration can lead to fatigue in the cable anchoring [3, 14, 20]. Various solutions have been developed to diminish cable vibration caused by wind or rain and wind combined. One approach is to utilize external dampers to enhance the damping of stay cables and subsequently mitigate stay cable vibration [21-24]. Concurrently, the other approaches employ alterations to the cable surface to enhance aerodynamic stability [25-29]. Helical fillets, and especially the narrow ones, are an effective method for lessening oscillations induced by rain and wind since they can prevent the creation of rain rivulets. In addition, they disrupted the flow, thereby reducing vibrations induced by vortices [25]. Authors in [25, 26] reported that the implementation of narrow helical fillets can effectively mitigate vibrations resulting from rain and wind and that appropriate helical fillet spacing is necessary to properly manage vibrations produced by rain and wind. Nevertheless, the surface pressure distribution characteristics of these cables did not yield any valuable information. Authors in [27] offered test examples demonstrating the effectiveness of helical fillets in preventing vibrations due to rain and wind. Authors in [28] conducted tests to visually demonstrate the patterns of flow in the cable wake using smoke visualizations. Remarkably, wind tunnel tests revealed that the presence of small diameter helical fillets effectively inhibited the axial-flow on the downwind side of the stay cable, particularly at lower wind velocities. The results showcased the efficacy of helical fillets in mitigating axial flow, a contributing factor to vibrations induced by rain and wind. Authors in [14] proposed the use of a large-sized helical fillet to reduce the occurrence of stay cable dry galloping. According to their research, it was found that the best size for a helical fillet to prevent dry galloping is approximately 1/15 of the cable diameter. This is observed at pitch pitches of two to three times the cable diameter, as evidenced in Figure 1 [14]. Nevertheless, the mitigating mechanism has not yet been elucidated.

Fig. 1. Helical fillet cable model.

More research is required to fully comprehend the helical fillet stay cables' suppression process. Further investigation is especially needed into the features of surface pressure distribution during the wind-induced vibration of circular cables and the way in which helical fillets prevent this from happening. Therefore, the use of wind tunnel testing to solve these concerns is the main goal of this work. Initially, both circular and helical fillet cables will have their wind-induced vibration under dry circumstances examined. The distribution of surface pressure during cable dry galloping will then be noted.

II. WIND-TUNEL EXPERIMENTS

A. Wind-Tunnel Test (WTT)

The trials were carried out at the wind-tunnel facility of Yokohama National University, Japan. The wind tunnel features a functional space with dimensions of 1.3 m in both width and height. The device has the capability to achieve a maximum wind speed of around 20 m/s, which corresponds to a Reynolds number of up to 10^5.

Figure 2 demonstrates the spring system utilized to support the cable models during testing. This arrangement enabled vertical oscillations to occur in a configuration with just one degree of freedom. This configuration was deployed to take the cable models through these tests. The studies were conducted using a uniform and steady flow, ensuring a turbulence intensity of 0.6% was maintained during the entire operation. The current wind tunnel test employed a stay cable model with a diameter of 86 mm and a Scruton number of 28.2. The cable model is configured with a yaw angle of 50°. The cable model system operates at a fundamental frequency of 1.72 Hz. The Scruton number is a dimensionless metric utilized to quantify the mass and damping characteristics of a bluff body in this table. In this study, the Scruton number was defined as:

$$S_c = \frac{2m\delta}{\rho D^2} \quad (1)$$

where δ is the logarithmic decrement of the cable model, ρ is the air density (kg/m^3), and m is the mass of the cable per unit length (kg/m).

Furthermore, the helical fillet model utilized identical dimensions with those of the circular cable. The size of the helical fillets is 1/15 times the diameter (D), while the pitch is twice the diameter ($2D$). Table I provides a comprehensive summary of the WTT parameters.

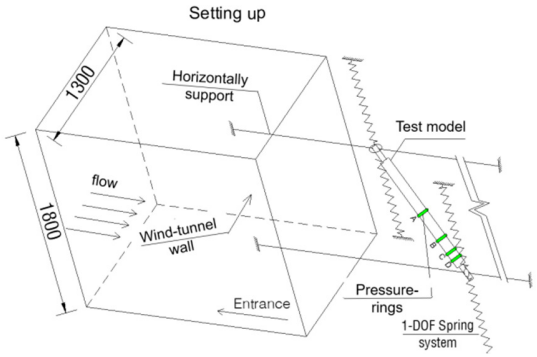

Fig. 2. Wind tunnel set-up.

TABLE I. WTT CONDITIONS

WTT specifications	Values
Cable diameter (D)	86 mm
Helical fillets size	1/15D
Helical fillets pitch	2D
Cable surfaces	Circular / Helical
Scruton number (Sc)	28.2
The fundamental frequency (Hz)	1.72
Reynolds number	0 – 10^5
Wind yaw angle	50°

B. Pressure Distribution Measurement and Analysis

Figure 2 illustrates the decomposition of the pressure measurement drawn up into its constituent pieces. A spring-supported system was employed to affix the experimental model at the entrance of the wind-tunnel. As a result, the surface pressure could be evaluated in a constantly fluctuating environment. To achieve precise surface pressure measurements, it was imperative to install pressure rings and taps on the cable model. The pressure rings were strategically placed at intervals from the cable end, namely 1*D* (Section D), 2*D* (Section C), *L*/4 (Section B), and *L*/2 (Section A). Each sector is allotted defined distances. Figure 3 illustrates that each ring is equipped with a combined total of 24 pressure taps. Specifically, the experiment's definition of the pressure holes' circumferential angle is the angle measured counterclockwise from the stagnation point.

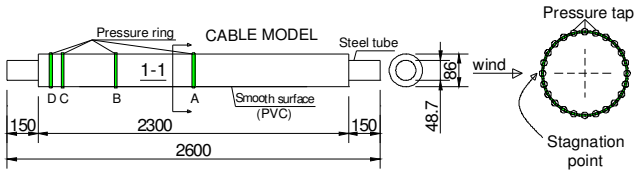

Fig. 3. Configuration of pressure sensors on cable prototype.

III. RESULTS AND DISCUSSION

A. Aerodynamic Performance of Circular Cable Surface and Helical Fillet Cables

Figure 4 compares a typical circular cable with a helical fillet cable, displaying the variations in their aerodynamic performance.

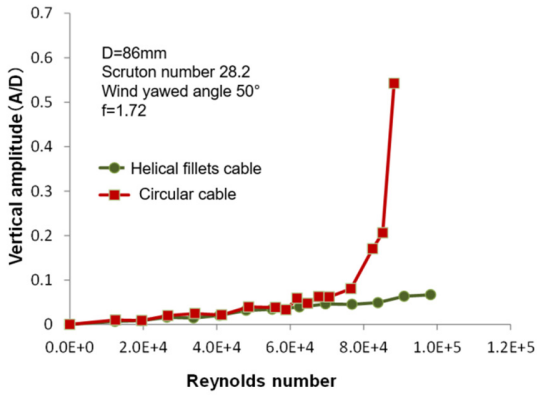

Fig. 4. Wind induced cable vibration with different surfaces.

At a Reynolds number of around 8.83×10^4, the occurrence of dry galloping becomes evident. This phenomenon has an oscillation amplitude that is about 0.6 times the diameter of the cable (0.6*D*). Furthermore, the stay cable continues to oscillate in a divergent manner, even while the wind speed remains constant. When it comes to decreasing cable vibration, the helical fillet cable stands out for its significantly enhanced efficacy. Remarkably, detrimental vibrations of a significant magnitude have been effectively averted thus far. Prior studies [12] have advocated for the use of larger helical fillets in cables to improve the occurrence of dry galloping. This observation aligns with the results of previous research.

B. Mean Pressure Coefficients of Circular Cables

A sub-critical Reynolds number of around 8.83×10^4 was seen to be the point at which dry galloping occurred, as was previously determined. The cable gradually began to display a propensity toward divergent galloping once it had transcended this significant barrier, even though the wind speed did not appear to increase substantially. A variety of surface pressure measurements were carried out with the utmost attention to detail to achieve the goal of gaining an all-encompassing comprehension of the complex properties of surface pressure distribution in this substantial range of Reynolds numbers. At Reynolds numbers of 8.83×10^4, 7.65×10^4, and 5.6×10^4 an evaluation was carried out and measurements were collected.

It is crucial to pay attention to the method used to measure pressure in these experiments. Pressures are often quantified according to the average static pressure inside the specific section of the wind tunnel being utilized for testing. Consequently, normalizing the observed pressures with respect to the average dynamic pressure noted over the testing time yields the pressure coefficients. Hence, the subsequent explanation provides a precise definition of the mean pressure coefficients:

$$C_{\bar{p}} = \frac{\frac{1}{T}\int_0^T p(t).dt}{q} \quad (2)$$

where: the function $p(t)$ represents the immediate pressure on the cable surface, T represents the time interval between each sample event, and t represents time (s). The expression $q=\frac{1}{2}\rho\bar{U}^2$ indicates the dynamic pressure exerted on the surface of the cable, where ρ represents the density of the air and U refers to the average wind speed.

Figures 5 to 8 depict the distribution of the average surface pressure (C_p) throughout various regions of the circular cable surface. The presence of a symmetrical distribution pattern is clearly apparent. Moreover, it is crucial to note that there is a substantial adverse pressure in regions where flow separation takes place, but a modest elevation in pressure may be observed on the side of the cable facing away from the wind. This phenomenon becomes more evident at Reynolds number values around 8.83×10^4.

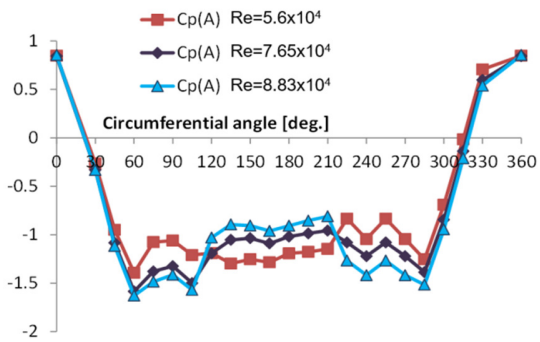

Fig. 5. Mean pressure coefficient at section A (circular cable).

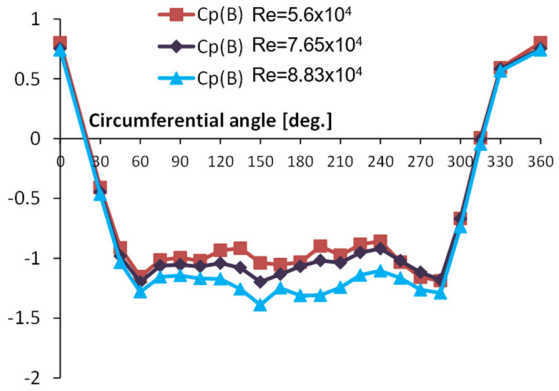

Fig. 6. Mean pressure coefficient at section B (circular cable).

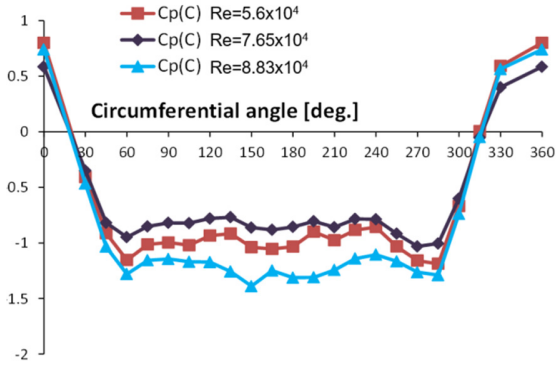

Fig. 7. Mean pressure coefficient at section C (circular cable).

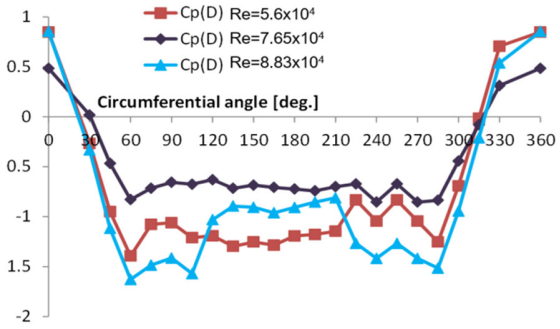

Fig. 8. Mean pressure coefficient at section D (circular cable).

By implementing an integration technique, the force coefficients at the central point, namely section A, were successfully obtained. This was achieved by considering the complete surface pressure distribution, which incorporated the cable model. Figure 9 discloses that when the Reynolds number increases, there is a significant reduction in the drag force coefficient. The decrease is most apparent when the yaw angle is around 50°. This reduction leads to a drag force coefficient of 0.4, which contributes to the production of the intended outcome, and it happens immediately prior to the onset of cable dry galloping.

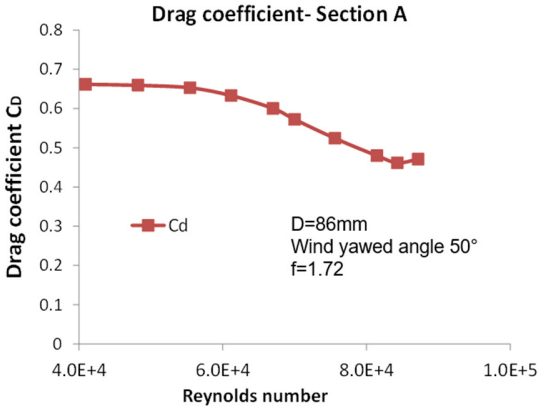

Fig. 9. Drag coefficient at section A.

C. Surface Pressure Redistribution for Helical Fillet Cables

Figure 10 provides details on the spatial arrangement of helical fillets in relation to the defined pressure measurement sections.

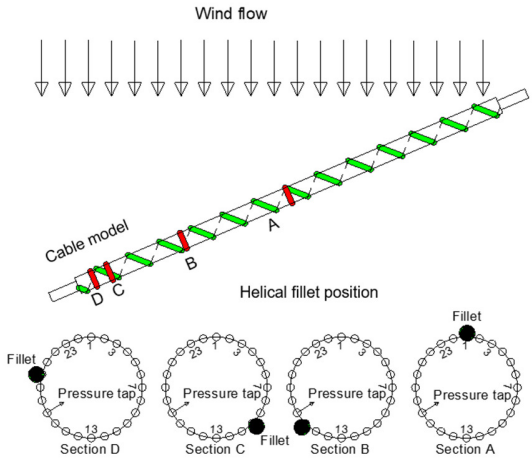

Fig. 10. Helical fillet position for each measurement section.

Figures 11-14 provide a complete illustration of the dispersion of the mean pressure coefficient of helical cables. Particularly noteworthy is the fact that the distribution of pressure coefficients is characterized by a noticeable asymmetry pattern. The mean surface pressure coefficient exhibits distinct zones that indicate an asymmetrical distribution: the upper half of the cable is marked by a predominance of positive pressure, whereas the lower half experiences a predominance of negative pressure. The surface pressure patterns display remarkable similarity throughout all four specified sections, despite the potential variations in the placement of the fillets. Incorporating a helical fillet in two dimensions leads to a notable reduction in the surface pressure on the underside of the item. This event emphasizes a subsequent rearrangement of surface pressure, leading to a departure from the typical pressure distribution observed in circular cables, as explained above. Especially, the discrepancy

in the results shown in Figures 13 and 14 at Re=7.51×10^4 can be due to encountering turbulent flow at this Reynolds number, along with the presence of the helical fillet. Turbulent flow involves increased mixing and velocity fluctuations compared to laminar flow at other Reynolds numbers. The helical fillet additionally affects flow dynamics, causing changes in pressure distribution and wake flow patterns.

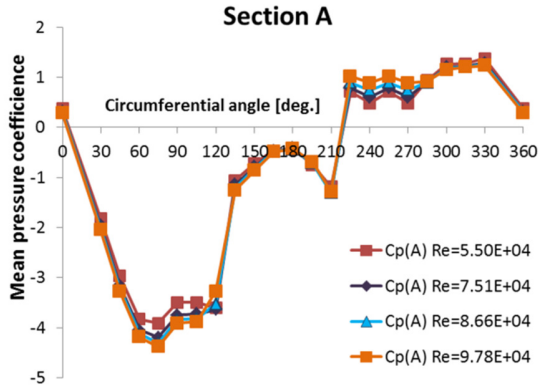

Fig. 11. Distribution of surface pressure in section A.

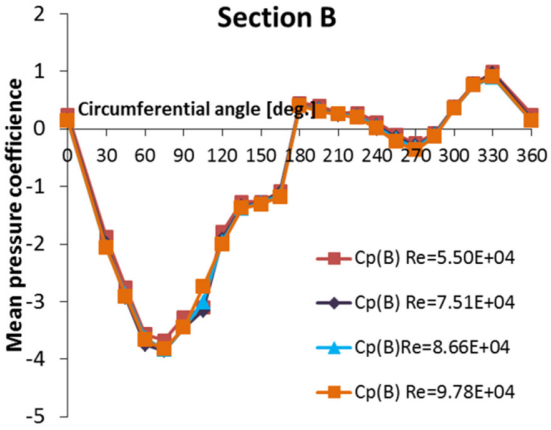

Fig. 12. Distribution of surface pressure in section B.

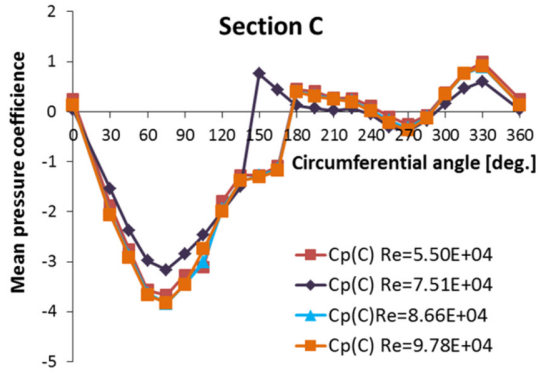

Fig. 13. Distribution of surface pressure in section C.

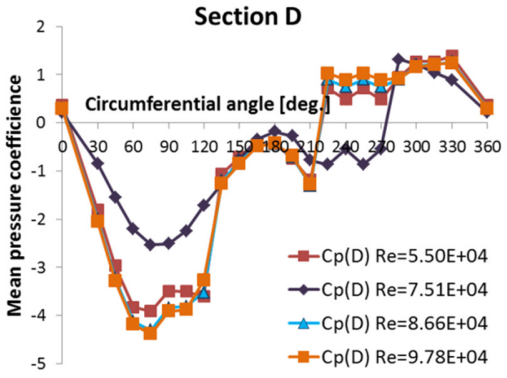

Fig. 14. Distribution of surface pressure in section D.

D. Wake Flow Structure

Figures 15 and 16 depict the Power Spectral Density (PSD) of the fluctuation in vertical velocity inside the wake flow of circular and helical cables.

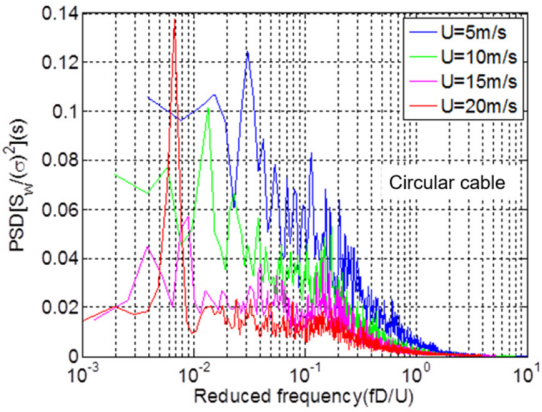

Fig. 15. PSD of the wake flow of circular cables.

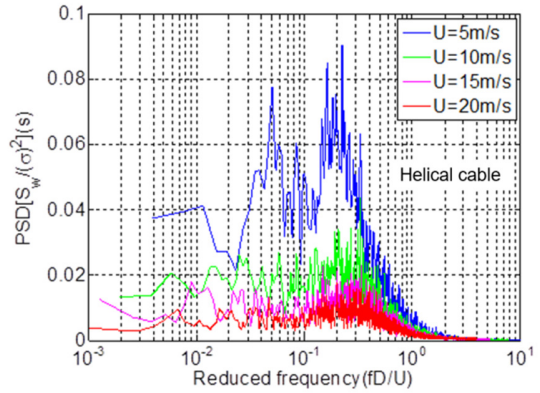

Fig. 16. PSD of the wake flow of helcial cables.

The measurement was performed at a location situated 2*D* behind the cable wake. Figure 15 depicts the PSD of the wake flow of a circular cable. In Figure 15, when the wind speed increases, the Karman Vortex PSD decreases. This demonstrates that the mitigation of Karman vortices results in

the cable becoming aerodynamically unstable [17]. Simultaneously, several prominent features of the PSD are observed in the low frequency components, corresponding to the frequencies associated with cable dry galloping. There is a concept proposing that when the Karman-vortex is suppressed, it disrupts the pattern of flow. This disruption leads to greater unpredictability of vortices along the axis of the stay cable. Consequently, this causes an increase in the PSD in the low frequency region. Conversely, when employing a helical fillet cable, the PSD of low frequency flow is suppressed as portrayed in Figure 16. In this case, the Karman-vortex at the Strouhal frequency (fD/U = 0.16 - 0.2) becomes dominant. When traditional Karman vortex sheds, dry galloping will not appear [34, 17]. Therefore, the suppression mechanism of helical fillet cable can be explained as follows: The presence of helical fillets ascertains that the flow remains regular even when wind speed rises, hence reducing the development of low frequency vortices, which are the major cause of cable dry galloping. Simultaneously, the Karman vortex becomes increasingly dominating, resulting in the absence of significant amplitude vibrations.

IV. CONCLUSIONS

To summarize, this wind tunnel study offers useful insights into the aerodynamic efficiency and pressure distribution on circular stay cables and helical fillet cables when subjected to wind. The study emphasizes notable disparities between the two cable types, namely regarding their stability and vulnerability to wind-induced vibrations. The study's findings may be summarized as:

- This study examines the influence of wind speed on the dynamics of cable vibration. It is suggested that increased wind speeds can lead to a cable instability phenomenon called dry galloping. On the other hand, helical fillet cables offer increased stability in the presence of strong winds, leading to an improved resistance to wind impact.
- Circular stay cables have symmetrical surface pressure distribution patterns, characterized by evenly distributed pressure magnitudes over their surfaces. However, under some wind conditions, cables may experience cable dry galloping, which indicates the possibility of instability. Helical fillet cables enhance stability in gusty situations by altering airflow patterns, resulting in an asymmetric distribution of surface pressure.
- Dry galloping in circular cables is caused by the elimination of Karman vortex and the existence of low-frequency components. The suppression mechanism of helical filet can be characterized as: The presence of helical fillets ensures a continuous and regular flow, even when wind speeds increase, hence reducing the occurrence of low frequency vortices. At the same time, the Karman vortex becomes the most important factor. As a result, the dry galloping is reduced.

ACKNOWLEDGEMENTS

This work was supported by The University of Danang, University of Science and Technology, code number of project: T2023-02-06.

REFERENCES

[1] J. P. Den Hartog, *Mechanical vibrations*, 4th ed. New York, NY, USA: McGraw-Hill, 1956.

[2] R. H. Scanlan, *Wind effects on structures: an introduction to wind engineering*. John Wiley & Sons, 1993.

[3] G. Larose and W. Smitt, "Rain/wind induced vibrations of parallel stay cables." in *Proceedings of the IABSE Conference, Cable-Stayed Bridges-Past, Present and Future*, Malmo, Sweden, 1999.

[4] D. Zuo and N. P. Jones, "Interpretation of field observations of wind- and rain-wind-induced stay cable vibrations," *Journal of Wind Engineering and Industrial Aerodynamics*, vol. 98, no. 2, pp. 73–87, Feb. 2010, https://doi.org/10.1016/j.jweia.2009.09.004.

[5] A. Bosdogianni and D. Olivari, "Wind- and rain-induced oscillations of cables of stayed bridges," *Journal of Wind Engineering and Industrial Aerodynamics*, vol. 64, no. 2, pp. 171–185, Nov. 1996, https://doi.org/10.1016/S0167-6105(96)00089-X.

[6] Y. Hikami and N. Shiraishi, "Rain-wind induced vibrations of cables stayed bridges," *Journal of Wind Engineering and Industrial Aerodynamics*, vol. 29, no. 1, pp. 409–418, Aug. 1988, https://doi.org/10.1016/0167-6105(88)90179-1.

[7] M. Aien, R. Ramezani, and S. M. Ghavami, "Probabilistic Load Flow Considering Wind Generation Uncertainty," *Engineering, Technology & Applied Science Research*, vol. 1, no. 5, pp. 126–132, Oct. 2011, https://doi.org/10.48084/etasr.64.

[8] M. Z. Abbasi, B. Noor, M. A. Aman, S. Farooqi, and F. W. Karam, "An Investigation of Temperature and Wind Impact on ACSR Transmission Line Sag and Tension," *Engineering, Technology & Applied Science Research*, vol. 8, no. 3, pp. 3009–3012, Jun. 2018, https://doi.org/10.48084/etasr.2046.

[9] H. Vo-Duy and C. H. Nguyen, "Mitigating Large Vibrations of Stayed Cables in Wind and Rain Hazards," *Shock and Vibration*, vol. 2020, May 2020, Art. no. e5845712, https://doi.org/10.1155/2020/5845712.

[10] D. Nguyen, H. Vo, H. Do, and M. Haque, "Optimization of Multiple Helical Fillets Surface to Suppress Rain-wind Vibration of Stay Cables: A Wind Tunnel Investigation," *The Open Civil Engineering Journal*, vol. 16, Sep. 2022, Art. no. e187414952206270, https://doi.org/10.2174/18741495-v16-e2206270.

[11] T. Saito, M. Matsumoto, and M. Kitazawa, "Rain-wind excitation on cable-stayed Higashi-Kobe bridge and cable vibration control," in *International Conference IABSE-FIP: Cable-stayed and suspension bridges*, Deauville, France, Oct. 1994, pp. 507–514.

[12] A. Honda, T. Yamanaka, T. Fujiwara, and T. Saito, "Wind tunnel test on rain-induced vibration of the stay-cable," in *International Symposium on Cable Dynamics*, Liege, Belgium, Oct. 1995, pp. 255–262.

[13] H. Katsuchi and H. Yamada, "Wind-tunnel Study on Dry-galloping of Indented-surface Stay Cable," in *11th Americas Conference on Wind Engineering*, San Juan, PR, USA, Jun. 2009, pp. 1–8.

[14] H. D. Vo, H. Katsuchi, H. Yamada, and M. Nishio, "A wind tunnel study on control methods for cable dry-galloping," *Frontiers of Structural and Civil Engineering*, vol. 10, no. 1, pp. 72–80, Mar. 2016, https://doi.org/10.1007/s11709-015-0309-7.

[15] V. D. Hung and N. D. Thao, "A Further Study on Stay Cable Galloping Under Dry Weather Condition," in *Innovation for Sustainable Infrastructure*, New York, NY, USA: Springer, 2020, pp. 191–196.

[16] K. Kleissl and C. T. Georgakis, "Aerodynamic control of bridge cables through shape modification: A preliminary study," *Journal of Fluids and Structures*, vol. 27, no. 7, pp. 1006–1020, Oct. 2011, https://doi.org/10.1016/j.jfluidstructs.2011.04.012.

[17] M. Matsumoto, T. Yagi, H. Hatsuda, T. Shima, M. Tanaka, and H. Naito, "Dry galloping characteristics and its mechanism of inclined/yawed cables," *Journal of Wind Engineering and Industrial Aerodynamics*, vol. 98, no. 6, pp. 317–327, Jun. 2010, https://doi.org/10.1016/j.jweia.2009.12.001.

[18] M. Matsumoto *et al.*, "Aerodynamic behavior of inclined circular cylinders-cable aerodynamics," *Journal of Wind Engineering and Industrial Aerodynamics*, vol. 33, no. 1, pp. 63–72, Mar. 1990, https://doi.org/10.1016/0167-6105(90)90021-4.

[19] S. Cheng, G. L. Larose, M. G. Savage, H. Tanaka, and P. A. Irwin, "Experimental study on the wind-induced vibration of a dry inclined cable—Part I: Phenomena," *Journal of Wind Engineering and Industrial Aerodynamics*, vol. 96, no. 12, pp. 2231–2253, Dec. 2008, https://doi.org/10.1016/j.jweia.2008.01.008.

[20] O. Rahat and I. Riazy, "Enhancing Transient Stability in Limited Variable Speed Induction Generator (Optislip) Based Wind Turbine (Case study: Binalood Wind Farm)," *Engineering, Technology & Applied Science Research*, vol. 6, no. 6, pp. 1280–1287, Dec. 2016, https://doi.org/10.48084/etasr.893.

[21] D.-T. Nguyen and D.-H. Vo, "A Study on Combination of Two Friction Dampers to Control Stayed-Cable Vibration Under Considering its Bending Stiffness," in *Innovation for Sustainable Infrastructure*, C. Ha-Minh, D. V. Dao, F. Benboudjema, S. Derrible, D. V. K. Huynh, and A. M. Tang, Eds. New York, NY, USA: Springer, 2020, pp. 87–92.

[22] D. T. Nguyen, D. H. Vo, and M. N. Haque, "Theoretical Investigation on the Impact of Two HDR Dampers on First Modal Damping Ratio of Stay Cable," *Applied Sciences*, vol. 11, no. 22, Jan. 2021, Art. no. 10985, https://doi.org/10.3390/app112210985.

[23] V. H. Cu and B. Han, "High-damping rubber damper for taut cable vibration reduction," *Australian Journal of Structural Engineering*, vol. 16, no. 4, pp. 283–291, Oct. 2015, https://doi.org/10.1080/13287982.2015.1092690.

[24] F. Di, L. Sun, and L. Chen, "Cable vibration control with internal and external dampers: Theoretical analysis and field test validation," *Smart Structures and Systems*, vol. 26, no. 5, pp. 575–589, Nov. 2020, https://doi.org/10.12989/sss.2020.26.5.575.

[25] O. Flamand, "Rain-wind induced vibration of cables," *Journal of Wind Engineering and Industrial Aerodynamics*, vol. 57, no. 2, pp. 353–362, Jul. 1995, https://doi.org/10.1016/0167-6105(94)00113-R.

[26] M. Gu and X. Du, "Experimental investigation of rain–wind-induced vibration of cables in cable-stayed bridges and its mitigation," *Journal of Wind Engineering and Industrial Aerodynamics*, vol. 93, no. 1, pp. 79–95, Jan. 2005, https://doi.org/10.1016/j.jweia.2004.09.003.

[27] R. S. Phelan, P. P. Sarkar, and K. C. Mehta, "Full-Scale Measurements to Investigate Rain–Wind Induced Cable-Stay Vibration and Its Mitigation," *Journal of Bridge Engineering*, vol. 11, no. 3, pp. 293–304, May 2006, https://doi.org/10.1061/(ASCE)1084-0702(2006)11:3(293).

[28] K. Kleissl and C. T. Georgakis, "Comparison of the aerodynamics of bridge cables with helical fillets and a pattern-indented surface," *Journal of Wind Engineering and Industrial Aerodynamics*, vol. 104–106, pp. 166–175, May 2012, https://doi.org/10.1016/j.jweia.2012.02.031.

[29] H. Wong, "An aerodynamic mean of suppressing vortex excited oscillation.," *Proceedings of the Institution of Civil Engineers*, vol. 63, no. 3, pp. 693–699, Sep. 1977, https://doi.org/10.1680/iicep.1977.3136.